Investigation of pre-cooling as a recommended measure to improve residential buildings' thermal resilience during heat waves

Zhaoyun Zeng, Wanni Zhang, Kaiyu Sun, Max Wei, Tianzhen Hong*

Building Technology and Urban Systems Division

Lawrence Berkeley National Laboratory, Berkeley, California, USA

*Corresponding author: thong@lbl.gov

Abstract

More intense heat waves are expected to occur more frequently in the twenty-first century. During severe heat waves, cooling capacity shortfall and overheating are likely to occur in residential buildings, and this will adversely affect occupant's thermal comfort and productivity. We propose a strategy of pre-cooling the house during off-peak hours to mitigate overheating during heat waves. Simulation results of a prototype single-family house show that adopting the rule-based control (RBC) of pre-cooling thermostat setpoint schedule is effective in reducing thermal discomfort, and that the efficacy of pre-cooling depends upon several building characteristics. An optimized control (OC) of the thermostat setpoint schedule was developed based on the simulation of a prototype building. A simplified yet improved RBC (IRBC) pre-cooling schedule was then extracted from the OC schedule for practical implementation at a larger scale. The effects of the RBC schedule and IRBC schedule were evaluated in the King District of Fresno, which contains 814 residential buildings. Results show that both thermostat setpoint schedules can reduce overheating effectively and that IRBC is slightly better than RBC for most buildings. The findings support the California government's recommendation on pre-cooling to mitigate overheating, which can be further improved with an optimized thermostat setpoint schedule broadcast to residents through early alert messages before a heat wave.

Keywords

Pre-cooling; Climate change; Thermal resilience; Heat wave; District-scale; Optimization

1. Introduction

As the climate changes, more intense heat waves are expected to occur with a higher frequency in the twenty-first century [1]. This poses a great threat to both the reliability of the grid and the well-being of residents [2]. On the grid side, heat waves prominently increase electricity generation costs and electricity demand, which may lead to the overheating of transmission lines and transformers and consequently large-scale power outages [3, 4]. Moreover, climate change is likely to increase the variability of temperature more prominently than its mean [5], indicating that the peak electricity demand is going to grow at a faster rate than that of total electricity consumption [6]. This presents a challenge to the construction and operation of the grid. On the resident side, heat waves are usually accompanied by a substantial number of heat-related deaths [7], especially in midlatitude regions [8, 9]. Some famous examples are the 1987 heat wave in Athens [10], the 1995 and 1999 heat waves in Chicago [8, 11], and the 2003 heat wave in Paris [12]. In addition to heat-related mortality and morbidity, heat waves also have a negative impact on the productivity of labor [13] and student learning [14]. Therefore, it is imperative that the government, utility companies, and residents all take their respective actions to address the challenges of climate change.

Since the growth rate of total electricity consumption is slower than that of peak electricity demand, it is uneconomic to invest in new electricity generation capacity and transmission network upgrades only to meet short-duration peak demand. Demand response (DR) is a much more cost-effective method to maintain the supply of and demand for electricity in balance. *Demand response* is the "changes in electric usage by end-use customers from their normal consumption patterns in response to changes in the price of electricity over time, or to incentive payments designed to induce lower electricity use at times of high wholesale market prices or when system reliability is jeopardized" [4]. Generally speaking, DR programs can be classified into incentive-based programs (IBP) and price-based programs (PBP) [4, 15]. IBP give customers incentives for their participation in the program or their load reduction performance. In some cases, the utility company has the ability to shut down remotely some of the participant's equipment on short notice. On the other hand, PBP regulate the customer's electric usage by means of dynamic electricity prices. The electricity price is generally higher in on-peak hours and lower in off-peak hours. PBP include the time-of-use (TOU) rate, critical peak pricing (CPP), extreme day pricing (EDP), extreme day CPP (ED-CPP), and real time pricing (RTP). With DR, the electricity demand curve in on-peak hours during heat waves hopefully can be flattened. In this way, the costs of generation capacity expansion and transmission network upgrades are avoided or deferred, the electricity generation cost is reduced (generation cost increases exponentially near maximum generation capacity), and the risk of power failure is decreased [4, 15].

From the residents' point of view, there are several ways to respond to dynamic electricity prices or load-reduction incentives. For example, residents can advance or defer the use of time-insensitive appliances, such as washing machines and electric dryers from on-peak hours to off-peak hours. This method is flexible, but its maximum load-shifting capability is limited [16]. The residents also can reduce the on-peak electricity consumption by raising the cooling setpoint (using a setback) during on-peak hours. This method has been proven effective in reducing electricity bills [17, 18], however, it is at the expense of the residents' thermal comfort [19].

The method with the greatest potential of on-peak electricity demand reduction is pre-cooling, which is to shift the on-peak cooling demand to off-peak hours by means of changing the cooling setpoints. Prior to the on-peak hours, the cooling setpoint is lowered below the normal level and cooling energy is stored in building thermal mass (including envelope thermal mass and internal thermal mass). During on-peak hours, the cooling setpoint is raised so the cooling energy stored in building thermal mass is gradually released while the cooling system is either inactive or running at lower power. There have been numerous studies on this topic that can be classified into rule-based control (RBC) studies [20-28] and optimized control (OC) studies [16, 25, 28-36]. These studies share two commonalities. First, pre-cooling performance is investigated in all normal weather conditions when the cooling capacity is sufficient. Since most cooling equipment is sized to meet the demand of 98.0%, 99.0%, or 99.6% of annual warm conditions [37], cooling capacity shortfall is going to occur during severe heat waves. Scientific evidence indicates that climate change results in not only a higher mean temperature in the future but also more occurrences of extreme weather [1, 5], which further increases the risk of cooling capacity shortfall. Second, all of these studies are economy-centric, i.e., they all focus on minimizing energy costs or peak electricity demand, while thermal comfort is used as a constraint and is compromised more or less. Some studies claim to be occupant-centric or that energy costs and thermal comfort are given equal weights, but actually the emphasis is still placed on energy costs. In [34], Li and Malkawi adopted both energy costs and thermal comfort as the objectives of a multi-objective optimization problem, but the weight of thermal comfort was varied to investigate how much energy costs can be reduced when the requirement on thermal comfort is relaxed. In [29], Erdinç et al. adopted thermal comfort as the objective function, but a stringent constraint was imposed on energy

costs. In essence, this study aims to optimize thermal comfort after an energy cost reduction goal has been achieved.

There are many ways to prevent the overheating of residential buildings when cooling capacity shortfall happens. The most straightforward way is of course to install or replace air conditioners with larger sizes. However, larger sizes entail additional expense, and partial load operation may degrade the efficiency of the cooling equipment [38, 39]. Another option is to retrofit the building envelope. By improving the insulation of the roofs or walls [40, 41], adopting cool roofs [42-45], or replacing existing windows with solar control or dynamic windows [46-53], the peak cooling demand, as well as annual cooling energy consumption, can be reduced, but the required investment may be substantial.

Previous studies have examined pre-cooling being adopted as a measure to reduce energy costs and peak electricity demand; this paper proposes that pre-cooling can be employed to improve the thermal resilience of residential buildings during heat waves. In this context, *pre-cooling* is defined as cooling the indoor air temperature to a few degrees lower than the conventional cooling setpoint in off-peak hours. As an improvement to previous works, we combined building-scale simulation with district-scale simulation to exploit both their advantages. Building-scale simulation requires less computational resources than district-scale simulation, which is suitable for parametric analysis and optimization. Results of district-scale simulation are more general, because a variety of buildings with different geometries and constructions are studied. The performance of RBC pre-cooling thermostat setpoint schedules and OC pre-cooling schedules are evaluated at two scales. The method proposed in this study could potentially be adopted by the government in developing optimized thermostat setpoint schedules and preparing early warning messages for the public prior to a heat wave [11, 54].

2. Methodology

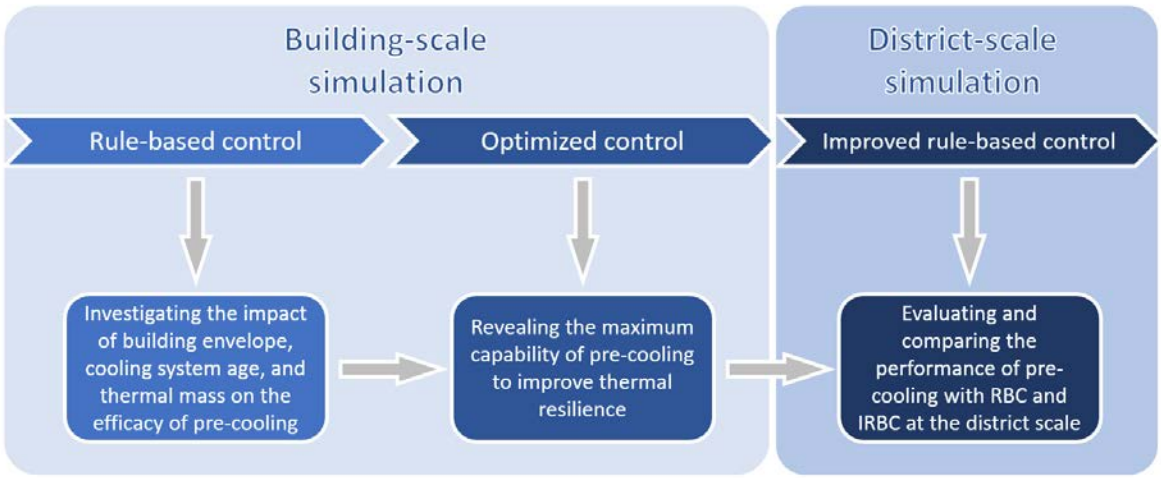

Figure 1 – The structure of this study

This study consisted of three primary steps. First, we implemented the RBC pre-cooling thermostat setpoint schedules in a residential prototype building as a demonstration of the effect of pre-cooling on thermal resilience. In this step, the impact of building envelope, cooling system age, and thermal mass on the efficacy of pre-cooling was also investigated by parametric analysis. These parameters were selected because they are crucial to the performance of pre-cooling [27]. Building envelope dictates the cooling load and the cooling system size, cooling system age affects the cooling capacity, and thermal mass determines

the thermal storage capacity. Second, we tried to explore the optimal cooling setpoint schedule of the prototype building to reveal the maximum capability of pre-cooling to improve thermal resilience. Since the OC schedule contains a unique setpoint for each control step, which is inconvenient to implement, a simplified RBC schedule with the key features of the OC schedule was extracted from it. We defined this extracted RBC schedule as the improved rule-based control (IRBC) schedule. Finally, the performance of the RBC pre-cooling schedule and the IRBC pre-cooling schedule was evaluated and compared at the district scale to assess the feasibility and effectiveness of applying the IRBC schedule, developed based on a single building, to a district. If the IRBC schedule proves to be more effective than the RBC schedule, it can be adopted by the local government in place of the latter as the recommended schedule and broadcast to residents through the early warning messages prior to a heat wave.

Building energy simulation (BES) in this study was conducted at two scales. Building-scale simulation was adopted in the first two steps for three reasons: (1) we could change the model for parametric analysis with less effort, (2) we could gain deeper insight into the effect of pre-cooling from the detailed temperature and energy profiles, and (3) the short simulation time of a simple building model allowed us to solve for the OC schedule with limited computational resources. District-level simulation was adopted in the last step for two reasons: (1) we could assess the feasibility and effectiveness of applying the IRBC schedule developed based on a single building to a district; and (2) the conclusions drawn from district-scale simulation are more general and consider the influence of diversity of the buildings in a residential district.

2.1 Metrics of overheating

We chose two thermal comfort metrics to evaluate the efficacy of precooling strategies. The first metric was a simple one, measuring the extent to which and the duration when indoor air temperature is above or below the comfort setpoint of the indoor air temperature. This is the so-called *unmet degree hours* (UDH). UDH was adopted because it is an indicator of the severity of cooling capacity shortfall during a heat wave. In essence, pre-cooling is utilizing the superfluous cooling capacity in off-peak hours to offset cooling capacity shortfall in on-peak hours. Hence, UDH is a good measure of the efficacy of pre-cooling. The second metric was based on predicted mean vote (PMV), called the *predicted mean vote exceedance hours* (PMVEH), to consider other thermal comfort factors including indoor air humidity, air velocity, occupant activity level, clothing level, and indoor surface radiant temperature. PMV is a thermal comfort index proposed by P. O. Fanger [55] that predicts the mean value of the thermal sensation votes (self-reported perceptions) of a large group of people. It has been adopted by various standards to evaluate the amenity of the thermal environment, such as ISO 7730 [56] and ASHRAE 55 [57]. This metric was adopted because, as discussed below, pre-cooling risks overcooling the building. PMVEH is able to measure the degree of overcooling, as well as the mitigation of overheating.

The UDH is defined as follows:

$$\mathrm{UDH} = \int_{t_1}^{t_2} \left[T(t) - T_{\mathrm{sp,b}}\right]_+ dt, \tag{1}$$

where

$$[x]_+ = \begin{cases} x, & x > 0 \\ 0, & x \leq 0 \end{cases},$$

T is the indoor air temperature [°C], $T_{\mathrm{sp,b}}$ is the baseline cooling setpoint [°C], and t is time [hr].

The second metric, PMVEH, is defined as follows:

$$\mathrm{PMVEH} = \int_{t_1}^{t_2} [|\mathrm{PMV}(t)| - \mathrm{PMV_{th}}]_+ \, dt, \tag{2}$$

where

$$[x]_+ = \begin{cases} x, & x > 0 \\ 0, & x \leq 0 \end{cases},$$

PMV is the predicted mean vote, and PMV_{th} is the PMV threshold of the comfort zone. This study adopted the comfort zone defined by ISO 7730, which is $-0.7 < PMV < +0.7$ [56]. Therefore, $PMV_{th} = 0.7$. In the calculation of PMV, the metabolic rate is 1.26 met, the clothing insulation is 0.5 clo, and the wind velocity is 0.2 m/s. PMVEH is mainly used in the objective function of OC. The reason for adopting PMVEH instead of UDH in OC is that UDH cannot measure the risk of overcooling.

2.2 Control strategies

The control strategies for heating, ventilation, and air conditioning (HVAC) thermostat setpoints can be categorized into RBC and OC. A rule-based controller adjusts the setpoint according to some basic rules or predetermined schedules [58]. RBC only requires simple thermostats and can be either manually or automatically implemented. Hence, it has been widely used in buildings. However, its performance is usually suboptimal. An optimized controller, on the other hand, adjusts the setpoint with an optimal or near-optimal control sequence obtained through the optimization of the simulated performance of a building [59]. Therefore, the performance of OC is usually superior to that of RBC. The optimization problem can be solved locally or on the cloud. The former requires a processor and sensors to measure weather variables, while the latter requires communication equipment and cloud services. Furthermore, a model needs to be created specifically for each building [60, 61]. These requirements limit the application of OC.

2.2.1 Rule-based control (RBC)

Three cooling setpoint schedules were tested in the RBC study, as shown in Figure 2. The baseline schedule is from the prototype residential building model created for the alternative calculation method testing of Title 24, Part 6, 2019 California Building Energy Efficiency Standards for Residential and Nonresidential Buildings (hereinafter referred to as Title 24) [62, 63], with a cooling setpoint of 25.56 °C (78 °F) and a setback of 28.33 °C (83 °F) on weekdays and a constant setpoint of 25.56 °C (78 °F) on weekends. The no-setback schedule is the baseline schedule without any setback (a 24-hour constant of 25.56 °C (78 °F)). The purpose of adding a setback is to reduce the cooling energy when the building is not occupied. However, the existence of a setback may aggravate overheating during on-peak hours, since the cooling system may not have sufficient capacity to cool the building down to the cooling setpoint from the higher setback temperature. The pre-cooling schedule was created according to a suggestion given by California State Senator Nancy Skinner prior to a heat wave in 2020 [64]. It has an off-peak pre-cooling setpoint of 22.22 °C (72 °F) and an on-peak cooling setpoint of 25.56 °C from 3:00 p.m. to 10:00 p.m.

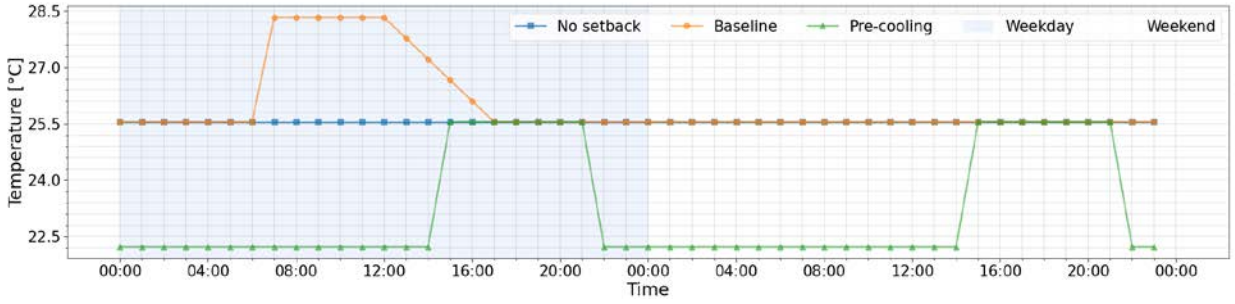

Figure 2 – The three RBC cooling setpoint schedules tested

2.2.2 Optimized control (OC)

The OC problem can be expressed in the following form [65]:

$$\text{Find } \mathbf{T}_{\text{sp}} = \begin{Bmatrix} T_{\text{sp},1} \\ T_{\text{sp},2} \\ \vdots \\ T_{\text{sp},n} \end{Bmatrix} \text{ which minimizes}$$

$$f(\mathbf{T}_{\text{sp}}) = w_1 \frac{\text{PMVEH}}{\text{PMVEH}_{\text{max}}} + w_2 \frac{M_{\text{HVAC}}}{M_{\text{HVAC}_{\text{max}}}}, \tag{3}$$

subject to

$$P_{cl} \leq P_{cl,max},$$

where $\mathbf{T}_{\text{sp}}$ is a n-dimensional vector containing the hourly cooling setpoint for the optimization horizon, and n depends on the length of the optimization horizon [°C]; w_1 and w_2 are two weighting factors; PMVEH is the total PMV exceedance hours during the heat wave [hr]; M_{HVAC} is the total cooling electricity cost during the heat wave [$]; $\text{PMVEH}_{\text{max}}$ and $M_{\text{HVAC}_{\text{max}}}$ are the maximum values of PMVEH and M_{HVAC} that may occur in optimization and are used to normalize PMVEH and M_{HVAC}; P_{cl} is the cooling power [W]; and $P_{cl,max}$ is the maximum cooling power of the cooling system [W]. This formulation aims to find the globally optimal hourly cooling setpoint sequence for the optimization horizon.

When the peak cooling load during a heat wave does not exceed the cooling capacity too much, pre-cooling is able to maintain the PMV within the comfort zone all the time. If the peak cooling load continues to grow, we may run into a situation where it requires deeper pre-cooling to reduce the peak cooling load but a lower pre-cooling setpoint will make the PMV in the pre-cooling period lower than –0.7, i.e., occupants may feel too cold. Therefore, we need to strike a balance between overheating and overcooling, which can be realized by minimizing the PMVEH.

The objective of this optimization problem is first to minimize the PMVEH of the building over the entire heat wave event. Only when this goal has been achieved, i.e., the PMVEH have been completely removed, is the secondary goal of minimizing the HVAC energy cost, it takes to remove the PMVEH, is taken into consideration. To achieve this objective, we need to ensure that w_1 $\text{PMVEH}/\text{PMVEH}_{\text{max}}$ is at least 5 times as large as w_2 $M_{\text{HVAC}}/M_{\text{HVAC}_{\text{max}}}$. Through trial and error, we found that a w_1 of 10 and a w_2 of 1 are a good choice.

The cooling electricity cost was calculated using the real electricity rate of the local utility company. The electricity provider of California, Pacific Gas and Electric (PG&E), provides a number of demand response plans to its customers. The final electricity rate depends on the type of plan the customer is enrolled in, the total monthly energy use, and the time of year. Here, we selected a simple TOU plan in which the off-peak rate and on-peak rate are $0.21122/kWh and $0.40489/kWh, respectively, and the on-peak hours are 4:00 p.m. to 9:00 p.m., as shown in Figure 3 [66].

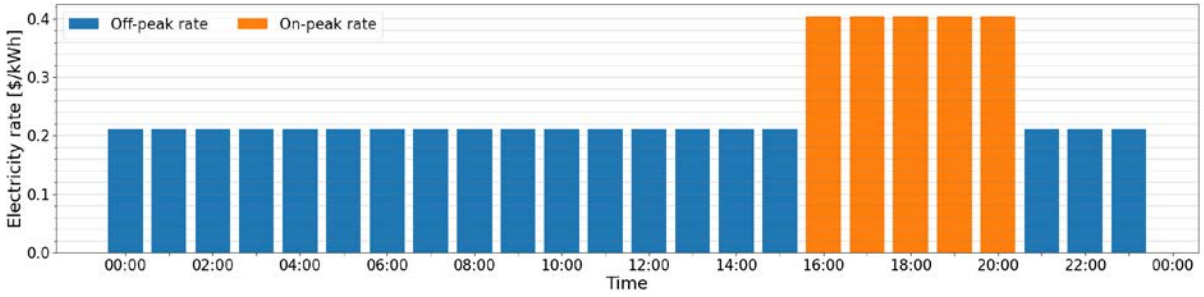

Figure 3 – The electricity rate used in this study

2.3 Building energy model

The building energy simulation (BES) program used in this study was EnergyPlus, a tool developed collaboratively by various U.S. national laboratories, academic institutions, and private firms and widely used both in academia and industry [67]. It has been extensively tested and validated [68].

The adopted prototype house in building-scale simulation was a one-story single-family building in California Climate Zone 13, represented by the city of Fresno. The building geometry is illustrated in Figure 4. The building model was originally created for the alternative calculation method testing of Title 24 [62]. Three vintages—1976, 2006, and 2015—were selected to represent buildings of different ages. The properties of the building model of a certain vintage comply with the version of Title 24 effective in that year (Title 24 is usually updated every three years) [63]. These properties are shown in Table 1. Since the first version of Title 24 was put into effect in 1978, the properties of the building model of 1976 vintage were chosen based on the assumptions presented by the 2019 Residential Compliance Manual for the 2019 Building Energy Efficiency Standards [69]. As Table 1 shows, the envelope of newer buildings has better insulation levels.

Fresno is a city located in the southern portion of California's Central Valley, as shown in Figure 5 (a). It has a Mediterranean climate with mild and wet winters and long, hot, dry summers. July is the warmest month, with a monthly average temperature of 26.9 °C [70].

Table 1 – The properties of the building models

Property	1976	2004	2015
Gross floor area [m²]	236		
Conditioned floor area [m²]	195 (garage is unconditioned)		
Window-to-wall ratio [-]	North: 0.2; Other orientations: 0.288		
Roof area [m²]	303		
Wall assembly U-factor [W/(m²·K)]	2.02	0.42	0.37
Wall cavity insulation [m²·K/W]	R0	R3.35	R2.64 cavity + R0.70 continuous
Top-floor ceiling cavity insulation [m²·K/W]	R1.94	R6.69	R6.69
Window thermal transmittance [W/(m²·K)]	3.69	3.69	1.82
Window SHGC [-]	0.4	0.4	0.25
Central AC: COP [-]	2.34	3.02	3.28
Gas furnace efficiency [-]	0.78	0.8	0.8
Gas water heater efficiency [-]	0.72	0.8	0.82
Lighting power density [W/m²]	6.25	3.07	1.95
Plug load power density [W/m²]	7.91	7.91	7.91

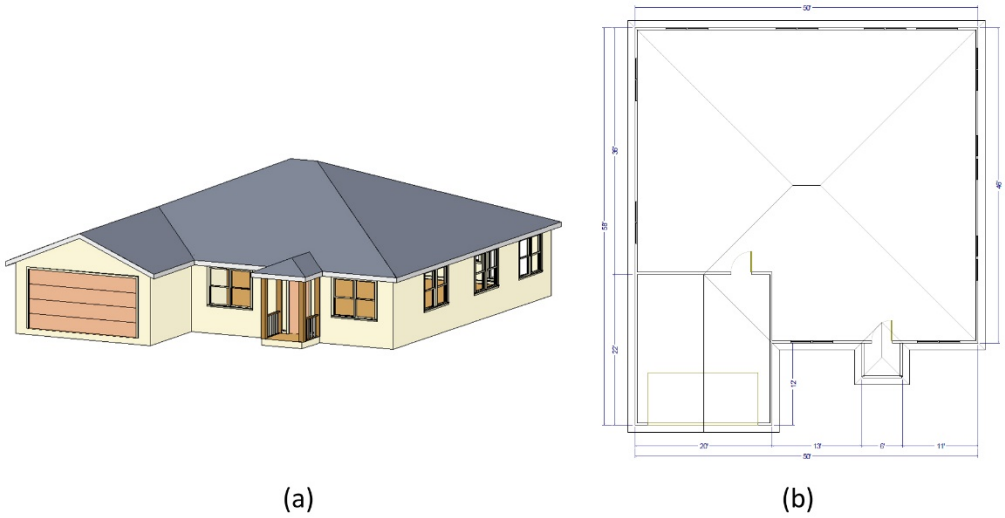

Figure 4 – (a) The front view of the prototype building; (b) The floor plan of the prototype building

CityBES was used for the district-scale modeling and analysis. CityBES is a web-based data and computing platform developed by Lawrence Berkeley National Laboratory that focuses on large-scale building energy modeling [71]. CityBES uses an international open data standard, CityGML, to represent and exchange three-dimensional city models and employs EnergyPlus as its BES engine. It provides a suite of functions for urban planners, building owners, utility company managers, energy consultants, and researchers.

The district simulated was the King District of the city of Fresno, as shown in Figure 5. The King District is a low-income district located to the southwest of Fresno's downtown that contains 480 single-family buildings and 334 multifamily buildings. The median household income of this district in 2019 is $20,850, about 30% of that of the entire United States. [72]. Therefore, the resilience measures that entail additional expense are likely to be unaffordable for the residents.

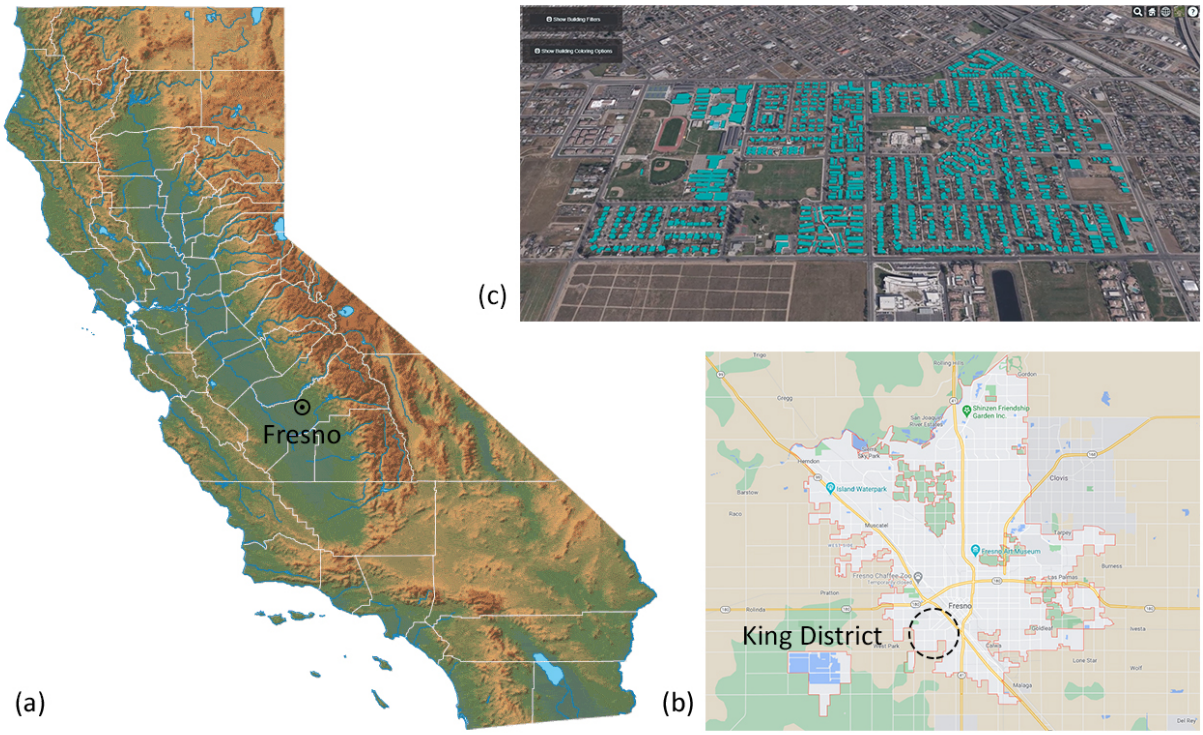

Figure 5 – (a) The location of Fresno in California; (b) The location of the King District in Fresno; (c) CityBES representation of the King District's building stock

2.4 Weather data

From July 22 to 26, 2006, Fresno was hit by a heat wave during which the daily maximum temperature exceeded 44 °C for five consecutive days. This is the most severe heat wave that Fresno has seen in the twenty-first century. The first two days were on weekends, and the last three days were on weekdays. Figure 6 shows the dry-bulb temperature and wet-bulb temperature of the five days. As a comparison, the dry-bulb temperature and wet-bulb temperature of the same days of the year from typical meteorological year 3 (TMY3) were also plotted [73]. It can be observed that the temperatures during the heat wave were prominently higher than those of a typical year. Although the dry-bulb temperature in the on-peak hours was not at its peak, the cooling load may have still been the highest, considering the delayed effect of the thermal mass, the increased internal load after the occupants return home, and the solar heat gain from west windows.

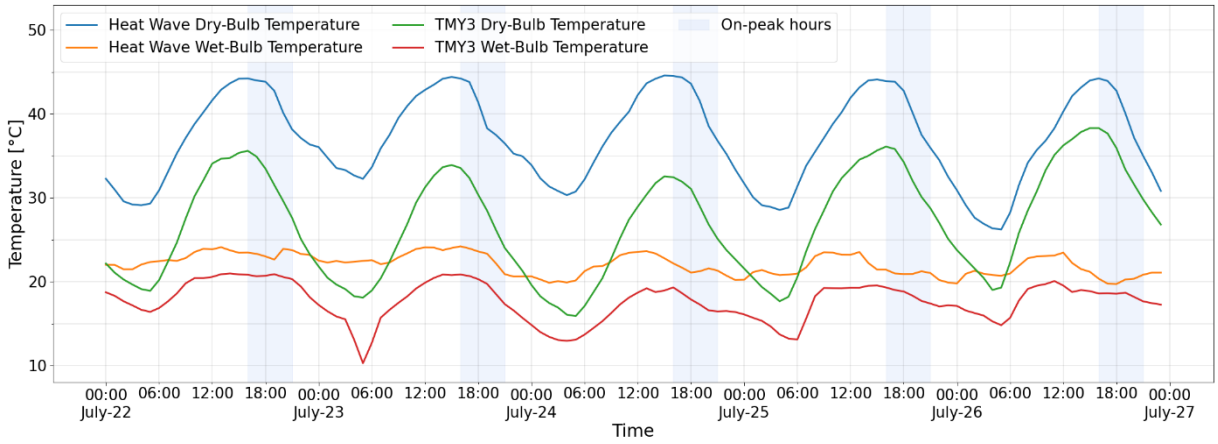

Figure 6 – Dry-bulb temperature profile and wet-bulb temperature profile during the heat wave

3. Simulation Results

3.1 Rule-based control

3.1.1 Effect of pre-cooling

In this section, the performance of the pre-cooling schedule is compared with that of the baseline schedule and the no-setback schedule. The temperature profiles and the hourly cooling electricity consumption profiles of the three schedules are shown in Figure 7 and Figure 8, respectively. The total UDH and the total cooling electricity cost of the three schedules are shown in Figure 9. For the readers' information, the PMV profiles of the three schedules are shown in Figure S1 in the appendix. The first two days were on weekends, so the temperature profiles of the baseline schedule and the no-setback schedule coincide. If we compare the three schedules within each vintage, we can see that both the no-setback schedule and the pre-cooling schedule can mitigate overheating effectively. The no-setback schedule reduced the total UDH by 16.5%, 21.5%, and 22.7% for buildings of 1976, 2004, and 2015 vintage, respectively. The values for pre-cooling were 58.2%, 64.2%, and 60.5%. Figure 8 shows that the cooling systems ran at full capacity from 12:00 p.m. to 18:00 p.m. no matter which schedule was adopted. Before and after this period of time, the hourly cooling electricity consumption of the pre-cooling schedule was much higher than that of the other two, which means the pre-cooling schedule exploited the excess cooling capacity during off-peak hours to pre-cool the building and stored the cooling energy in the thermal mass to counteract overheating during on-peak hours. Therefore, although the total cooling electricity consumption was increased, pre-cooling did not increase the peak cooling power or the on-peak cooling electricity consumption.

Compared to the great reduction of UDH, the cost increase was marginal. The additional cooling electricity costs of the five days of pre-cooling for the building of 1976, 2004, and 2015 vintage were $32.03, $18.86, and $13.48, respectively. Considering that pre-cooling is a provisional measure adopted only during heat waves, which usually last for only a few days each year, and that most heat waves are milder than this one, this additional cost would not be a heavy burden to King District residents.

Comparing the temperature profiles of different vintages, we can see that the indoor air temperature of older buildings was brought down to the pre-cooling setpoint faster than that of newer ones. This is because old buildings generally have larger HVAC systems, since the insulation of their envelope is worse. The auto-sized cooling capacities of the cooling coil for the buildings of 1976, 2004, and 2015 vintage are 14.65 kW, 8.57 kW, and 6.07 kW, respectively. Large cooling capacity is conducive to fast cooling of the building

during off-peak hours. For buildings of 1976 and 2004 vintage, we could defer lowering the cooling setpoint to 22.22 °C until the early morning to save energy.

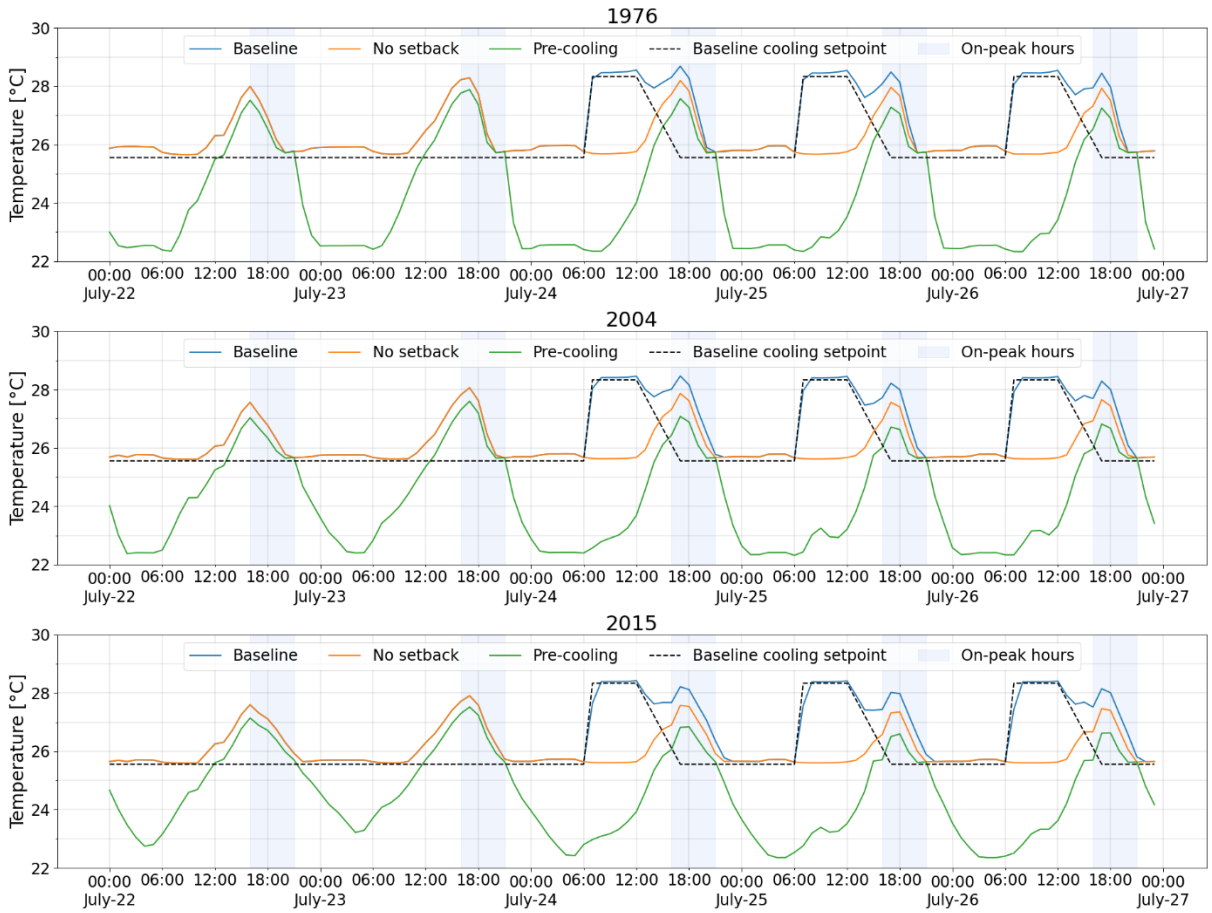

Figure 7 – The temperature profiles of the three cooling setpoint schedules during the heat wave

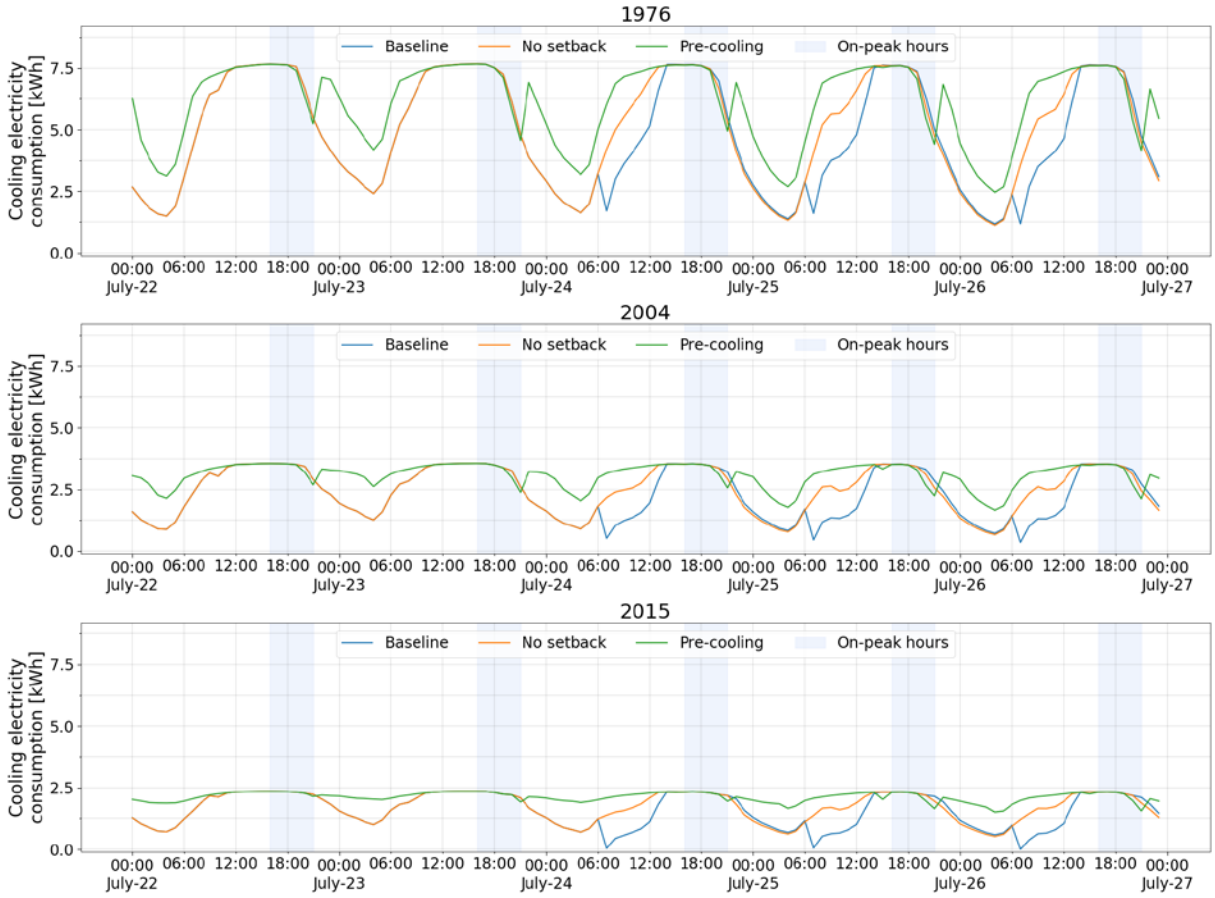

Figure 8 – The hourly cooling electricity consumption profiles of the three cooling setpoint schedules during the heat wave

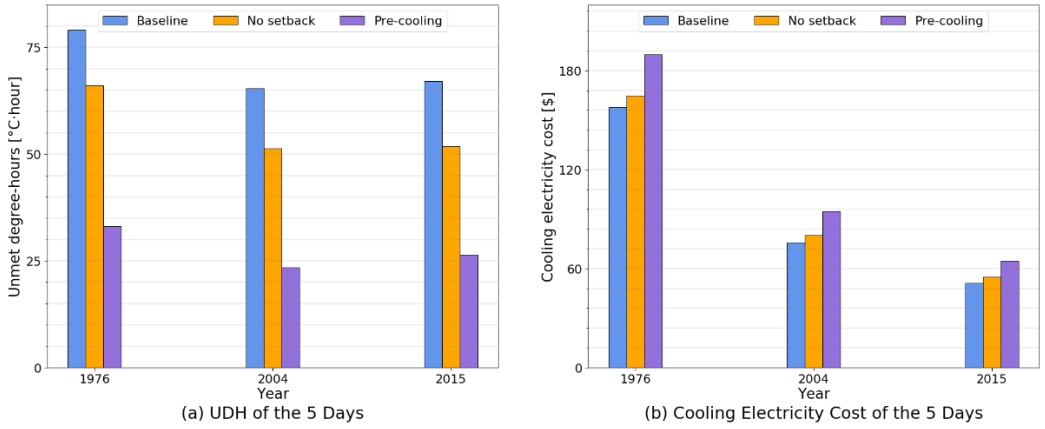

Figure 9 – (a) The total UDH and (b) the total cooling electricity cost of the three cooling setpoint schedules during the heat wave

3.1.2 Age of the cooling system

This section reviews the impact of the age of the cooling system on its performance during heat waves. Both the capacity and efficiency of HVAC systems degrade over time due to refrigerant leakage and coil fouling. Currently there is no consensus on the degradation rate of HVAC systems. We assume a

degradation factor of 2% per year for both the cooling capacity and the cooling efficiency (i.e., *coefficient of performance*, abbreviated COP) of the cooling equipment based on the data in the literature [74, 75].

Considering the service life of HVAC systems is usually 20 years [76], we tested four scenarios where the cooling system has been used for 0 (new), 5, 10, and 15 years. After 5, 10, and 15 years of service, the cooling capacity decreases to 90.4%, 81.7%, and 73.9% of the original value. The temperature profiles and total UDH of these scenarios are shown in Figure 10 and Figure 11, respectively. The PMV profiles of these scenarios are shown in Figure S2. Degradation of the cooling capacity not only aggravated overheating when the baseline schedule was adopted but also decreased the effectiveness of pre-cooling. For example, for a 1976 vintage building, pre-cooling could reduce the UDH of the baseline case by 58.2% when the cooling system was new. When the cooling system had been used for 15 years, the UDH of the baseline schedule increased by 123.8% and pre-cooling could only reduce the UDH of the baseline schedule by 24.1%. Moreover, newer buildings were more susceptible to the degradation of the cooling systems because of smaller cooling equipment sizes. For a 2015 vintage building, when the cooling system had been used for 15 years, pre-cooling had almost no effect on the indoor temperature in the first two days.

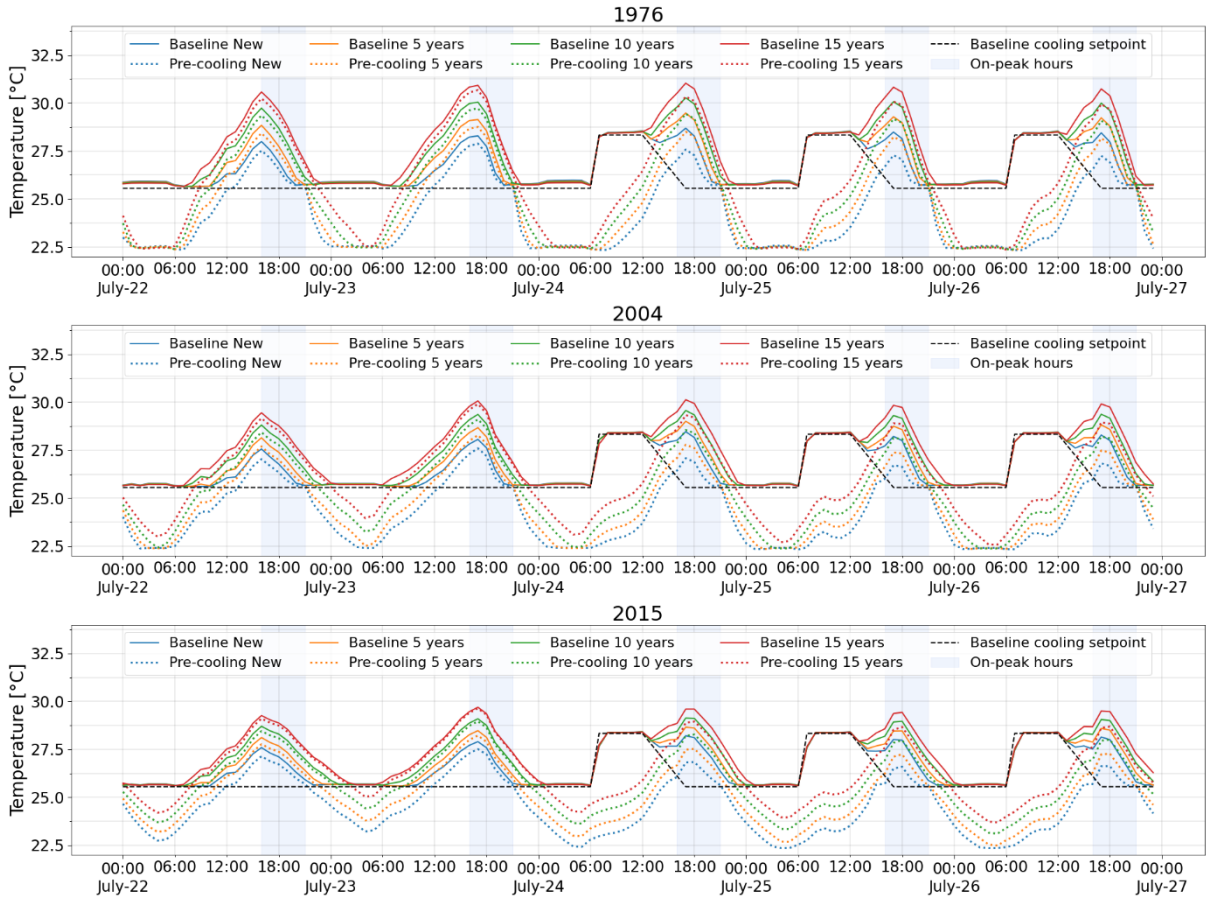

Figure 10 – The temperature profiles of cooling systems of different service time during the heat wave

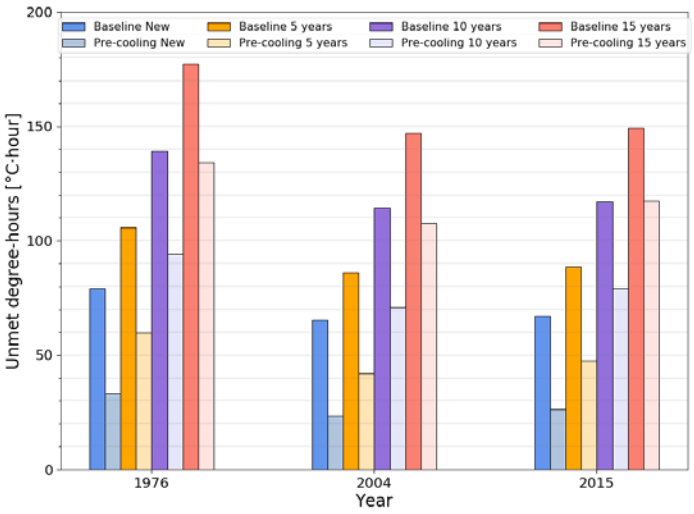

Figure 11 – The total UDH of cooling systems of different service time during the heat wave

3.1.3 Thermal mass of the building

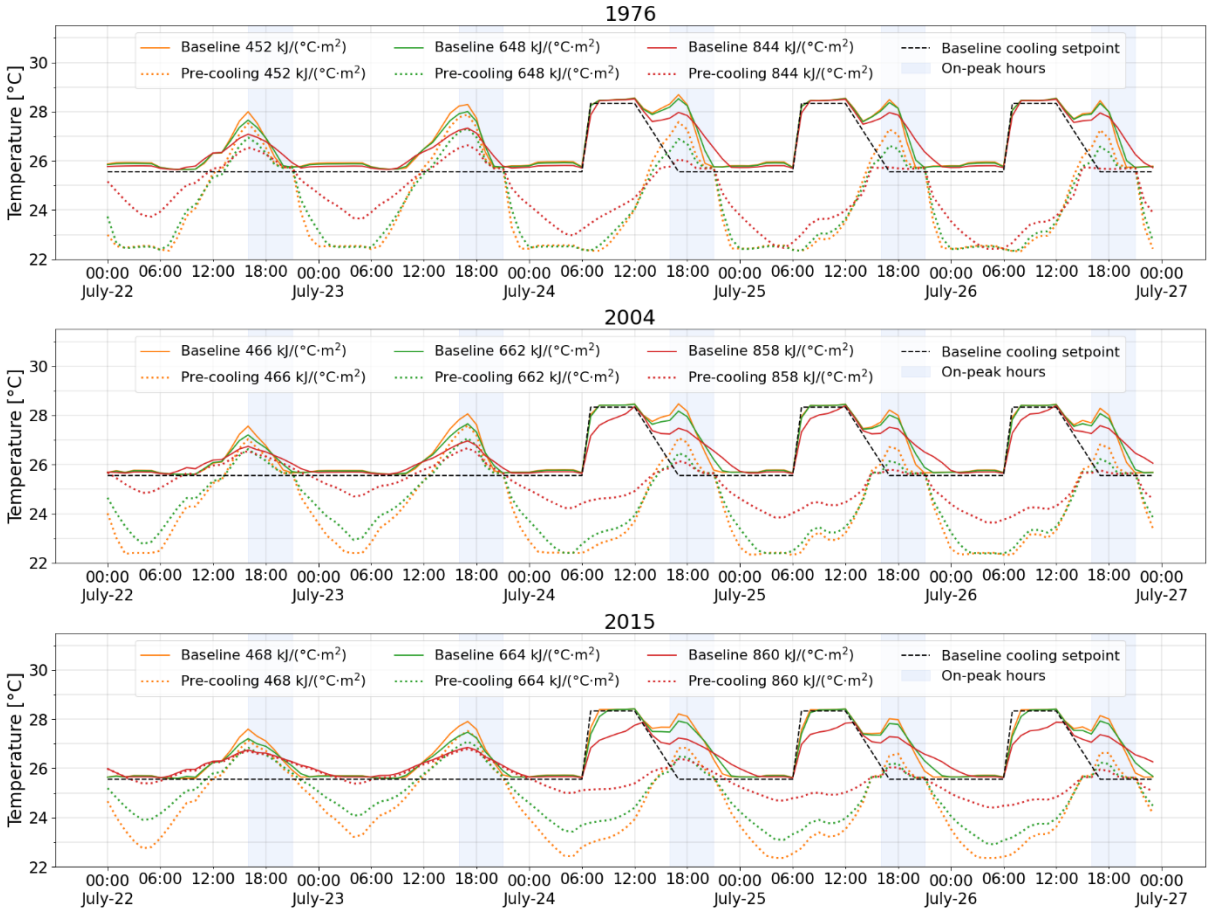

Figure 12 – The temperature profiles of buildings with different thermal mass during the heat wave

This section reviews the impact of building thermal mass on the effectiveness of pre-cooling. Only thermal mass of the conditioned zones was considered. The thermal mass of a building is comprised of two parts: the envelope thermal mass and the internal thermal mass. The envelope thermal mass of buildings of 1976, 2004, and 2015 vintage is 452 kJ/(°C·m^2), 466 kJ/(°C·m^2), and 468 kJ/(°C·m^2), respectively. The internal thermal mass, mainly the thermal mass of furniture and interior partition walls and doors, was assumed to be the same for buildings of all vintages with a value of 196 kJ/(°C·m^2). To study the impact of thermal mass on the effectiveness of pre-cooling, we created two more building models for each vintage whose envelope was unchanged but internal thermal mass was doubled and tripled, respectively. The temperature profiles and total UDH of buildings with different thermal mass are shown in Figure 12 and Figure 13, respectively. The PMV profiles of buildings with different thermal mass are shown in Figure S3.

For the baseline schedule, greater thermal mass led to smaller UDH. For the pre-cooling schedule, however, greater thermal mass was not always favorable. For the 1976 vintage building, since the cooling capacity was relatively large, greater thermal mass could store more cooling energy during the off-peak hours, which was conducive to the mitigation of overheating. When the internal thermal mass was tripled, pre-cooling was able to reduce the total UDH of the baseline schedule by 82.3%. For the buildings of 2004 and 2015 vintages, there was not enough cooling capacity to cool the thermal mass deep enough during the off-peak hours. Therefore, greater thermal mass cannot help store more cooling energy. On the contrary, it stores more heat during the on-peak hours for the cooling system to remove during the off-peak hours. Hence, the total UDH of the triple internal thermal mass case were even larger than those of the double internal thermal mass case.

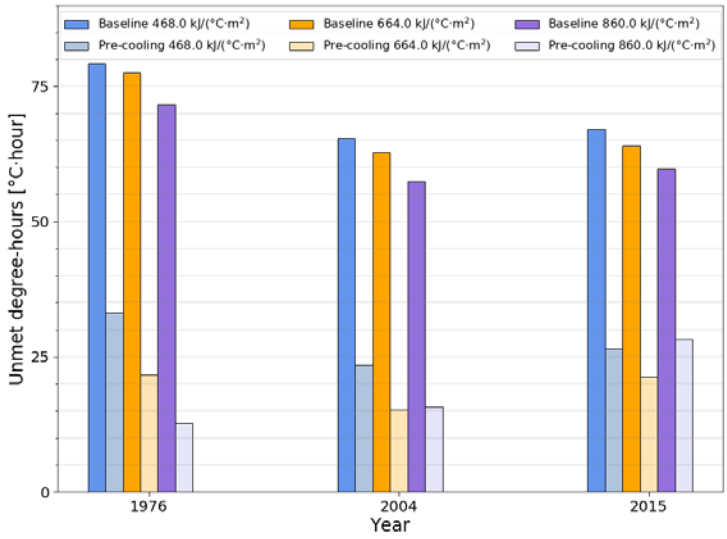

Figure 13 – The total UDH of buildings with different thermal mass during the heat wave

3.2 Optimized control

Next, the study tried to find the optimal cooling setpoint schedule through optimization. The heat wave of 2006 was comprised of five days with different temperature profiles. Ideally, a unique optimal hourly cooling setpoint schedule should be developed for each day, but this would result in a 120-dimension nonlinear optimization problem, which is beyond our capability to solve. Since the temperature profiles of the five days are not distinctly different from each other, we simplified the problem by using the same cooling setpoint schedule for the five days. In this case, the design variable was a 24-dimention vector with each element representing the cooling setpoint of one hour. The bounds for the cooling setpoint were [20.0,

28.33], where 20.0 °C was the heating setpoint (the cooling setpoint should never be lower than the heating setpoint) and 28.33 °C was the setback temperature of the baseline schedule. Considering the characteristics of this problem, we selected the differential evolution algorithms in the SciPy package of the Python language to solve it [77]. Differential evolution, developed by Storn and Price in 1997, is an effective algorithm for global optimization. It belongs to the class called *evolutionary algorithms*, which are population-based methods relying on mutation, recombination, and selection to evolve a collection of candidate solutions toward an optimal state [78]. A classical mutation constant (also known as *differential weight*) value of 0.5 and a classical recombination constant (also known as *crossover probability*) value of 0.7 were adopted. Based on the experience gained in the RBC simulations, we found that a $\mathrm{PMVEH}_{\max}$ of 40 hour and a $M_{\mathrm{HVAC}_{\max}}$ of \$200 could successfully constrain $\mathrm{PMVEH}/\mathrm{PMVEH}_{\max}$ and $M_{\mathrm{HVAC}}/M_{\mathrm{HVAC}_{\max}}$ within [0, 1].

For optimization, this study used a building vintage of 1976, because it represents the vintage of the majority of buildings in the King District. For buildings of that age, the HVAC systems usually have already been replaced at least once. Since there was no way for us to know when the cooling systems were replaced, we assumed on average the current cooling system had been used for 10 years. The RBC schedule and the OC schedule found in the optimization problem are shown in Figure 14. Since the OC schedule has a unique cooling setpoint for each hour, which is inconvenient to implement, we extracted an IRBC schedule from it to avoid frequent setpoint adjustment, as shown in Figure 14. We extract the IRBC schedule from the OC schedule considering that if the cooling setpoint fluctuates slightly around a temperature for a few hours (e.g., 1:00–7:00 and 14:00–18:00) or a few adjacent cooling setpoints are close to each other, we choose their mean value or an integer close to their mean value. The temperature and PMV profiles of the representative building using the three pre-cooling schedules are shown in Figure 15. By pre-cooling the building to a deeper level, both the OC schedule and the IRBC schedule was able to reduce the overheating slightly. The total PMVEH of the representative building using the RBC schedule, OC schedule, and IRBC schedule were 29.24 hours, 27.99 hours, and 28.19 hours, respectively. A PMVEH reduction of 3.59% was achieved by adopting the IRBC schedule compared to the RBC schedule. The total cooling electricity costs of this representative building of the RBC case, OC case, and IRBC case were \$204.14, \$208.79, and \$209.30, respectively.

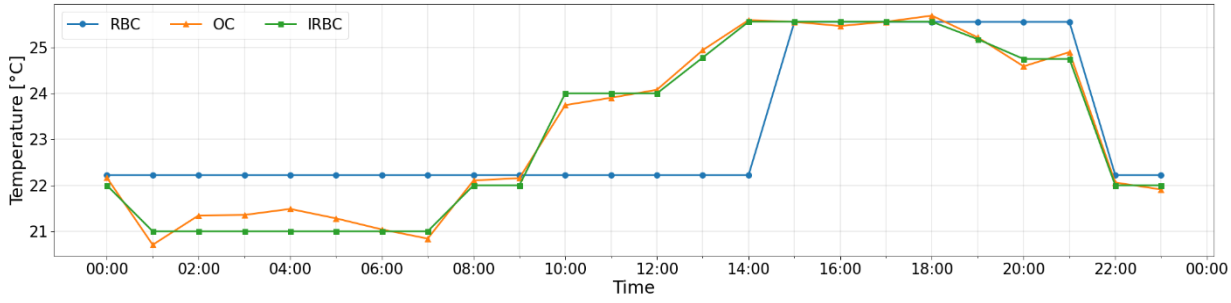

Figure 14 – The RBC schedule, OC schedule, and IRBC schedule

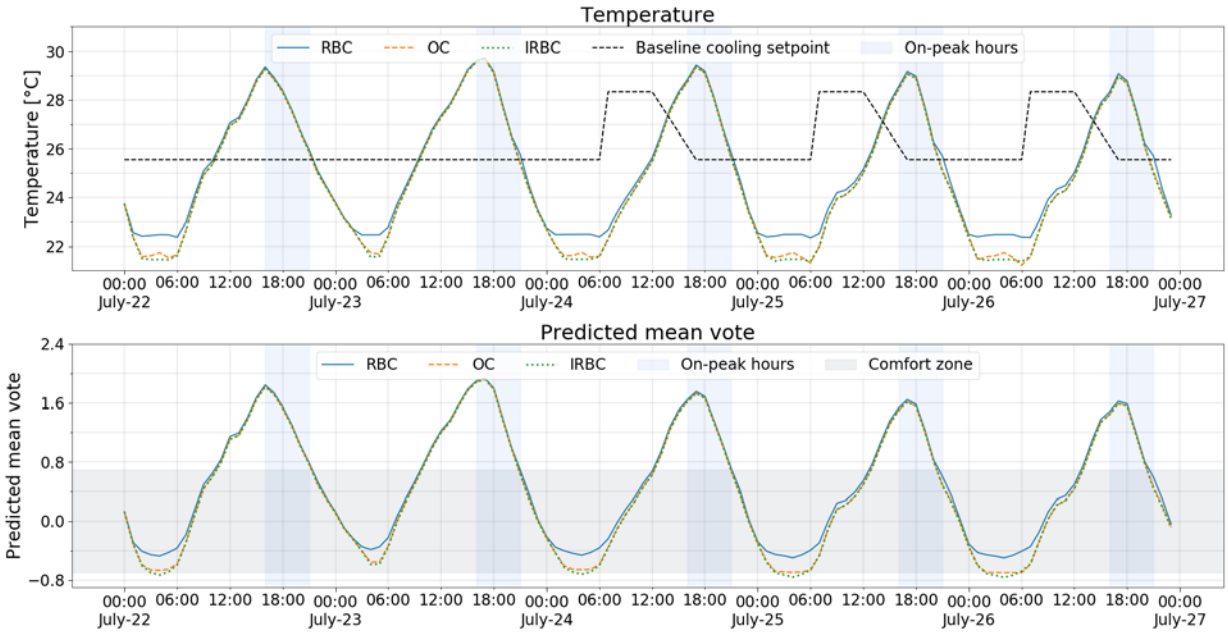

Figure 15 – The temperature and PMV profiles of the three pre-cooling schedules

3.3 District level simulation

This section compares the performance of the RBC schedule and the IRBC schedule at the district scale. The reason for doing this is that the IRBC schedule was developed based on the optimization of a small single-family building of 1976 vintage with a 10-year-old cooling system. The optimality of the schedule only applies to this building. Figure 16 shows that the King District is home to a wide variety of residential buildings (480 single-family buildings and 334 multifamily buildings), the vintages of which range from 1910 to 2014, and total floor area range from 54 m^2 to 987 m^2. The IRBC schedule may be advantageous for some buildings but disadvantageous for the others.

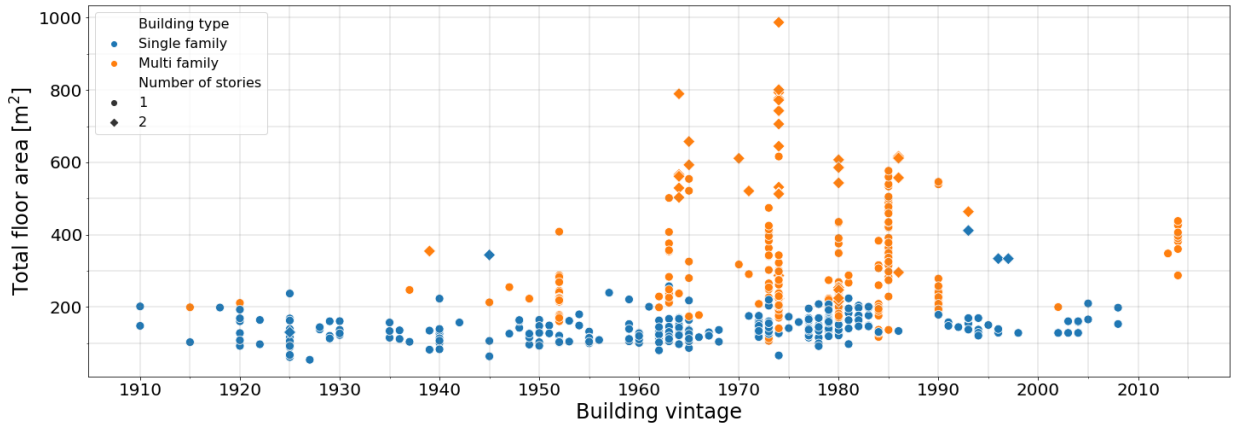

Figure 16 – The characteristics of buildings in the King District

Figure 17 shows the UDH, PMVEH, and cooling electricity costs of all residential buildings in the King District by using three different cooling schedules. The box in the box-whisker plot denotes the first and third quartiles of the value of all buildings. The horizontal line in the middle of the box denotes the median. The upper whisker denotes the value equal to $Q_3 + 1.5(Q_3 - Q_1)$, where Q_3 and Q_1 are the third and first

quartiles. The lower whisker denotes the value equal to $Q_1 - 1.5(Q_3 - Q_1)$. Both the RBC pre-cooling schedule and the IRBC pre-cooling schedule can reduce the median UDH from 148 °C·hr to about 110 °C·hr. The PMVEH of the buildings were reduced from 47 hrs to about 26 hrs. The performance of IRBC seems slightly better than that of RBC. The median cost of RBC was $14.2 higher than that of the baseline and the median cost of IRBC was $2.2 higher than that of RBC.

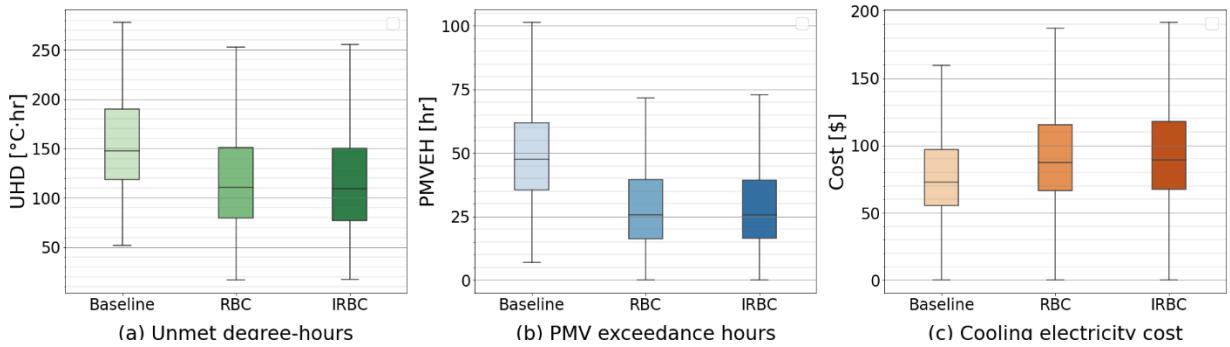

Figure 17 – The (a) UDH, (b) PMVEH, and (c) cooling electricity cost of all residential buildings in the King District by using three different cooling schedules

To closely compare the effects of RBC and IRBC, we also plotted the percentage of reduction of the UDH, PMVEH, and cost of IRBC relative to RBC. Of the buildings studied, 96.8% had a positive UDH reduction, and the median UDH reduction was 0.77%. Although the reduction was small for most buildings, a few buildings achieved decent UDH reductions by adopting IRBC, the maximum of which was 11.0%. Of the buildings studied, 76.4% had a positive PMVEH reduction, but the median PMVEH reduction was only 0.04%. The reduction of PMVEH was smaller than that of UDH because some buildings were overcooled, and their PMVEH were increased. Of all the buildings studied, 87.7% had a negative cost reduction, and the median cost reduction was –1.52%. In conclusion, the overheating of most buildings was mitigated more or less by adopting the IRBC schedule instead of the RBC schedule, but the degree of improvement was usually marginal.

Therefore, if a local government has sufficient computational resources and detailed information about the local building stock, it would be worth developing an exclusive IRBC schedule for each category of buildings and broadcasting these IRBC schedules as recommended thermostat setpoint schedules in the early warning messages prior to a heat wave. If not, the RBC schedule provided by California State Senator Nancy Skinner is good enough for most buildings [62].

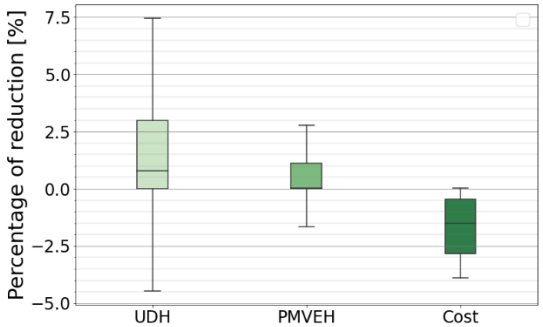

Figure 18 – The percentage of reduction of the UDH, PMVEH, and cost of IRBC relative to RBC

4. Discussion

This paper evaluates the effectiveness of employing pre-cooling to mitigate overheating risk during heat waves at both the building scale and the district scale, considering the diversity of the building stock in age, size, and efficiency level. Although the building data and building code are based on Fresno, California, and California Building Energy Efficiency Standards Title 24, the method is applicable to other cities and countries as long as their local building stock, building energy efficiency standards, weather data, and utility rates are used. The findings and recommendations are applicable to all local governments and utilities where the majority of residential buildings are equipped with active cooling systems.

There are two major limitations of this simulation-based study. First, due to the limited time and resources, the efficacy of pre-cooling is only evaluated in one heat wave; the efficacy of pre-cooling may be different in heat waves with different duration and intensity. Second, the King District is representative of most suburban residential districts in the United States where single-family buildings and small multifamily buildings constitute the majority of the buildings. However, in urban districts of big cities, the majority of buildings are high-rise apartments and large commercial buildings. For high-rise apartments, the large thermal mass and central air-conditioning systems make the application of pre-cooling quite different from that in single-family buildings and small multifamily buildings.

During heat waves, peak electricity demand increases dramatically, which leads to a high risk of power outages. If most residents are willing to sacrifice their thermal comfort somewhat by raising the cooling setpoint by a few degrees (e.g., to 30 °C or 32 °C), peak electricity demands can be significantly reduced [79] and the risk of power outages can be mitigated. This is an interesting research topic for us in the future.

5. Conclusions

This study employed building performance simulation to investigate the effectiveness of adopting pre-cooling thermostat setpoint schedules during heat waves to improve occupants' thermal comfort. The main findings are as follows:

- Both the no-setback schedule and the pre-cooling schedule can mitigate overheating effectively compared with the baseline schedule during heat waves. In particular, pre-cooling can reduce the total UDH by about 60% at the expense of an additional cooling electricity cost ranging from $13.48 to $32.03 for a household.
- Older buildings tend to have cooling systems with larger capacity that is sized for larger cooling loads due to less insulated envelope. Cooling systems with larger capacity can cool the indoor air temperature faster to the pre-cooling setpoint and hence have better pre-cooling effects. Degradation of the cooling system not only aggravates overheating when the baseline schedule is adopted but also decreases the effectiveness of pre-cooling. Newer buildings are more susceptible to the degradation of the cooling systems because of smaller cooling equipment sizing. With more frequent and more intense heat waves, cooling systems need to be sized considering future climate to ensure adequate capacity for cooling during heat waves.
- When the baseline schedule is adopted, greater building thermal mass leads to smaller UDH. When the pre-cooling schedule is adopted, greater building thermal mass is only favorable when the cooling capacity is sufficiently large.
- An optimized thermostat setpoint schedule was developed based on the prototype building, and a simplified IRBC schedule was extracted from the OC schedule. The performance of the RBC schedule and the IRBC schedule was evaluated at the district scale. Both schedules are effective in

mitigating overheating in the district and the IRBC schedule is slightly better than the RBC schedule for most buildings.

- If the local government or utility company has sufficient computational resources and detailed information about the local building stock, it would be worth developing an exclusive optimized thermostat setpoint schedule for each major category of building stock and broadcasting these recommended schedules through the early warning messages to residents prior to a heat wave. Otherwise, the improved rule-based thermostat setpoint schedule is adequate for most residential buildings, balancing thermal comfort and utility cost.

Acknowledgments

This research was supported by the California Strategic Growth Council under Contract CCR0047, and by the U.S. Department of Energy's Building Technologies Office under Contract No. DE-AC02-05CH11231. We thank Elizabeth Grassi and Leah Fisher, managers of the California Strategic Growth Council, for their feedback and support.

References

1. Meehl, G.A. and C. Tebaldi, *More Intense, More Frequent, and Longer Lasting Heat Waves in the 21st Century*. Science, 2004. **305**(5686): p. 994.
2. Mora, C., et al., *Global risk of deadly heat.* Nature Climate Change, 2017. **7**(7): p. 501-506.
3. Ke, X., et al., *Quantifying impacts of heat waves on power grid operation.* Applied Energy, 2016. **183**: p. 504-512.
4. U.S. Department of Energy, *Benefits of demand response in electricity markets and recommendations for achieving them*. 2006.
5. Schär, C., et al., *The role of increasing temperature variability in European summer heatwaves.* Nature, 2004. **427**(6972): p. 332-336.
6. Dirks, J.A., et al., *Impacts of climate change on energy consumption and peak demand in buildings: A detailed regional approach.* Energy, 2015. **79**: p. 20-32.
7. Kovats, R.S. and S. Hajat, *Heat Stress and Public Health: A Critical Review.* Annual Review of Public Health, 2008. **29**(1): p. 41-55.
8. Kalkstein, L.S., *Lessons from a very hot summer.* Lancet, 1995. **346**(8979): p. 857-859.
9. Chestnut, L.G., et al., *Analysis of differences in hot-weather-related mortality across 44 U.S. metropolitan areas.* Environmental Science & Policy, 1998. **1**(1): p. 59-70.
10. Katsouyanni, K., et al., *THE 1987 ATHENS HEATWAVE.* The Lancet, 1988. **332**(8610): p. 573.
11. Palecki, M.A., S.A. Changnon, and K.E. Kunkel, *The Nature and Impacts of the July 1999 Heat Wave in the Midwestern United States: Learning from the Lessons of 1995.* Bulletin of the American Meteorological Society, 2001. **82**(7): p. 1353-1368.
12. Le Tertre, A., et al., *Impact of the 2003 Heatwave on All-Cause Mortality in 9 French Cities.* Epidemiology, 2006. **17**(1): p. 75-79.
13. Zander, K.K., et al., *Heat stress causes substantial labour productivity loss in Australia.* Nature Climate Change, 2015. **5**(7): p. 647-651.
14. Park, R.J., A.P. Behrer, and J. Goodman, *Learning is inhibited by heat exposure, both internationally and within the United States.* Nature Human Behaviour, 2020.
15. Albadi, M.H. and E.F. El-Saadany, *A summary of demand response in electricity markets.* Electric Power Systems Research, 2008. **78**(11): p. 1989-1996.
16. Perez, K.X., M. Baldea, and T.F. Edgar, *Integrated HVAC management and optimal scheduling of smart appliances for community peak load reduction.* Energy and Buildings, 2016. **123**: p. 34-40.

17. Moon, J.W. and S.-H. Han, *Thermostat strategies impact on energy consumption in residential buildings.* Energy and Buildings, 2011. **43**(2): p. 338-346.
18. Nik, V.M. and A. Moazami, *Using collective intelligence to enhance demand flexibility and climate resilience in urban areas.* Applied Energy, 2021. **281**: p. 116106.
19. Surles, W. and G.P. Henze, *Evaluation of automatic priced based thermostat control for peak energy reduction under residential time-of-use utility tariffs.* Energy and Buildings, 2012. **49**: p. 99-108.
20. Reddy, T.A., L.K. Norford, and W. Kempton, *Shaving residential air-conditioner electricity peaks by intelligent use of the building thermal mass.* Energy, 1991. **16**(7): p. 1001-1010.
21. Xu, P., et al. *Peak demand reduction from pre-cooling with zone temperature reset in an office building*. in *ACEEE 2004 Summer Study on Energy Efficiency in Buildings*. 2004. Asilomar, Pacific Grove, CA.
22. German, A. and M. Hoeschele, *Residential mechanical precooling*. 2014, U.S. Department of Energy.
23. Morgan, S. and M. Krarti, *Impact of electricity rate structures on energy cost savings of pre-cooling controls for office buildings.* Building and Environment, 2007. **42**(8): p. 2810-2818.
24. Arababadi, R., *Developing and modeling potential precooling strategies for residential buildings in the Phoenix climate.* ASHRAE Transactions, 2015. **121**(1).
25. Keeney, K.R. and J.E. Braun, *Application of building precooling to reduce peak cooling requirements.* ASHRAE Transactions, 1997. **103**(1): p. 463-469.
26. Yin, R., et al., *Study on Auto-DR and pre-cooling of commercial buildings with thermal mass in California.* Energy and Buildings, 2010. **42**(7): p. 967-975.
27. Katipamula, S. and N. Lu, *Evaluation of Residential HVAC Control Strategies for Demand Response Programs.* ASHRAE Transactions, 2006. **112**(1).
28. Wang, J., C.Y. Tang, and L. Song, *Design and analysis of optimal pre-cooling in residential buildings.* Energy and Buildings, 2020. **216**: p. 109951.
29. Erdinç, O., et al., *End-User Comfort Oriented Day-Ahead Planning for Responsive Residential HVAC Demand Aggregation Considering Weather Forecasts.* IEEE Transactions on Smart Grid, 2017. **8**(1): p. 362-372.
30. Keeney, K. and J. Braun, *A Simplified Method for Determining Optimal Cooling Control Strategies for Thermal Storage in Building Mass.* HVAC&R Research, 1996. **2**(1): p. 59-78.
31. Ali, M., A. Safdarian, and M. Lehtonen. *Demand response potential of residential HVAC loads considering users preferences*. in *IEEE PES Innovative Smart Grid Technologies, Europe*. 2014.
32. Alibabaei, N., et al., *Effects of intelligent strategy planning models on residential HVAC system energy demand and cost during the heating and cooling seasons.* Applied Energy, 2017. **185**: p. 29-43.
33. Lee, K.-h. and J.E. Braun, *Model-based demand-limiting control of building thermal mass.* Building and Environment, 2008. **43**(10): p. 1633-1646.
34. Li, X. and A. Malkawi, *Multi-objective optimization for thermal mass model predictive control in small and medium size commercial buildings under summer weather conditions.* Energy, 2016. **112**: p. 1194-1206.
35. Braun, J.E., *Reducing energy costs and peak electrical demand through optimal control of building thermal storage.* ASHRAE Transactions, 1990. **96**(2): p. 876-888.
36. Avci, M., M. Erkoc, and S.S. Asfour. *Residential HVAC load control strategy in real-time electricity pricing environment*. in *2012 IEEE Energytech*. 2012.
37. American Society of Heating Refrigerating and Air-Conditioning Engineers, *2013 ASHRAE Handbook: Fundamentals*. 2013, ASHRAE: Atlanta, GA.
38. Li, Y., et al., *A novel method to determine the motor efficiency under variable speed operations and partial load conditions.* Applied Energy, 2015. **144**: p. 234-240.
39. Waddicor, D.A., et al., *Partial load efficiency degradation of a water-to-water heat pump under fixed set-point control.* Applied Thermal Engineering, 2016. **106**: p. 275-285.

40. Aktacir, M.A., O. Büyükalaca, and T. Yılmaz, *A case study for influence of building thermal insulation on cooling load and air-conditioning system in the hot and humid regions.* Applied Energy, 2010. **87**(2): p. 599-607.
41. Cheung, C.K., R.J. Fuller, and M.B. Luther, *Energy-efficient envelope design for high-rise apartments.* Energy and Buildings, 2005. **37**(1): p. 37-48.
42. Suehrcke, H., E.L. Peterson, and N. Selby, *Effect of roof solar reflectance on the building heat gain in a hot climate.* Energy and Buildings, 2008. **40**(12): p. 2224-2235.
43. Levinson, R., et al., *Inclusion of cool roofs in nonresidential Title 24 prescriptive requirements.* Energy Policy, 2005. **33**(2): p. 151-170.
44. Akbari, H., et al., *Peak power and cooling energy savings of high-albedo roofs.* Energy and Buildings, 1997. **25**(2): p. 117-126.
45. Dabaieh, M., et al., *Reducing cooling demands in a hot dry climate: A simulation study for non-insulated passive cool roof thermal performance in residential buildings.* Energy and Buildings, 2015. **89**: p. 142-152.
46. Gasparella, A., et al., *Analysis and modelling of window and glazing systems energy performance for a well insulated residential building.* Energy and Buildings, 2011. **43**(4): p. 1030-1037.
47. Lee, E.S., et al., *A design guide for early-market electrochromic windows*. 2006, Lawrence Berkeley National Laboratory: Berkeley, California, USA.
48. Lee, E.S. and A. Tavil, *Energy and visual comfort performance of electrochromic windows with overhangs.* Building and Environment, 2007. **42**(6): p. 2439-2449.
49. Papaefthimiou, S., E. Syrrakou, and P. Yianoulis, *Energy performance assessment of an electrochromic window.* Thin Solid Films, 2006. **502**(1): p. 257-264.
50. Apte, J., D. Arasteh, and Y.J. Huang. *Future advanced windows for zero-energy homes*. in *ASHRAE Transactions*. 2003.
51. Dussault, J.-M., L. Gosselin, and T. Galstian, *Integration of smart windows into building design for reduction of yearly overall energy consumption and peak loads.* Solar Energy, 2012. **86**(11): p. 3405-3416.
52. Baetens, R., B.P. Jelle, and A. Gustavsen, *Properties, requirements and possibilities of smart windows for dynamic daylight and solar energy control in buildings: A state-of-the-art review.* Solar Energy Materials and Solar Cells, 2010. **94**(2): p. 87-105.
53. Sun, K., et al., *Passive cooling designs to improve heat resilience of homes in underserved and vulnerable communities.* Energy and Buildings, 2021: p. 111383.
54. Lowe, D., K.L. Ebi, and B. Forsberg, *Heatwave Early Warning Systems and Adaptation Advice to Reduce Human Health Consequences of Heatwaves.* International Journal of Environmental Research and Public Health, 2011. **8**(12): p. 4623-4648.
55. Fanger, P.O., *Thermal comfort. Analysis and applications in environmental engineering*. 1970: Copenhagen: Danish Technical Press. 244 pp.
56. International Organization for Standardization, *ISO 7730: Ergonomics of the thermal environment — Analytical determination and interpretation of thermal comfort using calculation of the PMV and PPD indices and local thermal comfort criteria*. 2005, ISO.
57. American Society of Heating Refrigerating and Air-Conditioning Engineers, *ANSI/ASHRAE Standard 55-2017: Thermal Environmental Conditions for Human Occupancy*. 2017, ASHRAE, Inc.: Atlanta, Ga.
58. Favoino, F., et al., *Optimal control and performance of photovoltachromic switchable glazing for building integration in temperate climates.* Applied Energy, 2016. **178**: p. 943-961.
59. Favoino, F., Q. Jin, and M. Overend, *Design and control optimisation of adaptive insulation systems for office buildings. Part 1: Adaptive technologies and simulation framework.* Energy, 2017. **127**: p. 301-309.
60. Killian, M. and M. Kozek, *Ten questions concerning model predictive control for energy efficient buildings.* Building and Environment, 2016. **105**: p. 403-412.

61. Henze, G.P., *Modeling and simulation in building automation systems*, in *Building Performance Simulation for Design and Operation*. 2019, Taylor & Francis Group: London, UK.
62. California Energy Commission, *2019 Alternative Calculation Method Approval Manual*. 2018.
63. California Energy Commission, *2019 Building Energy Efficiency Standards for Residential and Nonresidential Buildings*. 2018.
64. Skinner, N. *Staying Cool and Reducing Electricity Use*. 2020; Available from: https://sd09.senate.ca.gov/sites/sd09.senate.ca.gov/files/e_alert/20200817_SD09_information_670.htm?utm_campaign=nancy-skinner-staying-cool-and-reducing-electricity-use&utm_medium=email&utm_source=information&utm_content=websitefooter.
65. Marler, R.T. and J.S. Arora, *Survey of multi-objective optimization methods for engineering.* Structural and Multidisciplinary Optimization, 2004. **26**(6): p. 369-395.
66. Pacific Gas and Electric Company. *PG&E's Time-of-Use rate plans*. 2021; Available from: https://www.pge.com/en_US/residential/rate-plans/rate-plan-options/time-of-use-base-plan/time-of-use-plan.page.
67. U.S. Department of Energy, *EnergyPlus™ Version 8.6 Documentation -- Engineering Reference*. 2016.
68. U.S. Department of Energy. *Testing and Validation | EnergyPlus*. 2015; Available from: https://energyplus.net/testing.
69. California Energy Commission, *2019 Residential Compliance Manual for the 2019 Building Energy Efficiency Standards*. 2018.
70. Climate-Data.org. *Fresno Climate (United States of America)*. 2021; Available from: https://en.climate-data.org/north-america/united-states-of-america/california/fresno-764460/.
71. Chen, Y., T. Hong, and M.A. Piette, *Automatic generation and simulation of urban building energy models based on city datasets for city-scale building retrofit analysis.* Applied Energy, 2017. **205**: p. 323-335.
72. U.S. Census Bureau. *Median Income in the Past 12 Months (In 2019 Inflation-Adjusted Dollars)*. 2021; Available from: https://data.census.gov/cedsci/table?q=s1903&g=0500000US06019.140000&tid=ACSST5Y2019.S1903&hidePreview=false.
73. Wilcox, S. and W. Marion, *Users Manual for TMY3 Data Sets*. 2008, National Renewable Energy Laboratory.
74. Hendron, R., *Building America Performance Analysis Procedures for Existing Homes*. 2006, National Renewable Energy Laboratory.
75. Parker, D. and K. Fenaughty, *Evaluation of air conditioning performance degradation: Opportunities from diagnostic methods*, in *2018 ACEEE Summer Study on Energy Efficiency in Buildings*. 2018.
76. Taylor, M. *HVAC System Life Cycles: How Long Should They Really Last?* 2019; Available from: https://www.achrnews.com/articles/140416-hvac-system-life-cycles-how-long-should-they-really-last.
77. The SciPy Community. *scipy.optimize.differential_evolution — SciPy v1.6.1 Reference Guide*. 2021 Feb 18, 2021; Available from: https://docs.scipy.org/doc/scipy/reference/generated/scipy.optimize.differential_evolution.html#scipy-optimize-differential-evolution.
78. Price, K.V., *Differential Evolution*, in *Handbook of Optimization*, I. Zelinka, V. Snášel, and A. Abraham, Editors. 2013, Springer: Berlin, Heidelberg.
79. Wang, Z., et al., *Predicting city-scale daily electricity consumption using data-driven models.* Advances in Applied Energy, 2021. **2**: p. 100025.